Supplemental Methods

Data Acquisition

All subjects were scanned on a 3T Magnetic resonance scanner (EXCITE, General Electric, Milwaukee, USA). High-resolution T1-weighted volumetric 3D images were obtained using a spoiled gradient recall (SPGR) sequence (TR=8·5 ms, TE=3·4 ms, flip angle=12°, slice thickness=1 mm) with an 8-channel phased-array head coil. A field of view (FOV) of 240×240 mm^2 was used, with an acquisition matrix comprising 256 readings of 128 phase-encoding steps and an in-plane resolution of 0·47×0·47 mm^2.

Amplitudes of low-frequency (0·01–0·08 Hz) fluctuations (ALFF) of the blood oxygenation level-dependent (BOLD) signal were obtained using a gradient-echo echo-planar imaging (EPI) sequence (TR/TE=2000/30 ms; flip angle=90°). The slice thickness was 5 mm (no slice gap), with a matrix size of 64×64 and a FOV of 240×240 mm^2, resulting in a voxel size of 3·75×3·75×5 mm^3. Each brain volume was comprised of 30 axial slices, and each functional run contained 200 image volumes. Seven patients and 7 controls with excessive head motion (translation more than 1·5mm or rotation more than 1·5°) were excluded, resulting in samples of 100 patients and 100 controls in statistical analyses.

Voxel-Based Morphometry Analysis

VBM analyses of T1 MR images were performed using Statistical Parametric Mapping (SPM8; http://www.fil.ion.ucl.ac.uk/spm) and the VBM8 toolbox (http://dbm.neuro.uni-jena.de/vbm). This approach facilitates an optimal segmentation and registration of Magnetic Resonance Imaging (MRI) scans to the standardized anatomical space of the Montreal Neurological Institute (MNI). In brief, T1 images were bias-corrected and segmented to gray matter, white matter and cerebrospinal fluid using a customized template which was constructed from our 200 study participants. An automated brain extraction step was incorporated in order to eliminate voxels from non-gray matter structures with signal intensities similar to gray matter, such as the dural venous sinuses, scalp, cranial marrow, and diplopic space. Then gray matter partitions were spatially normalized (using a 12-parameter affine transformation and 7×8×7 nonlinear basis functions) to the created customized gray matter template. The deformation parameters obtained from the normalization process were applied to each participant's original raw image (in native space) in order to create optimally normalized whole brain images, which were recursively segmented for brain tissue extraction. Finally, the segmented images were modulated with the Jacobian determinants derived from spatial normalization (1) and smoothed with an isotropic Gaussian kernel with full-width at half-maximum (FWHM) of 6 mm.

ALFF Calculation

The ALFF was calculated using Data Processing Assistant for Resting-State fMRI (DPARSF) MATLAB toolbox (http://www.restfmri.net). In brief, after converting DICOM files to NIFTI images, the first 5 time points were discarded. Then slice timing and head motion correction were performed. The data were then normalized to MNI space by using standard EPI template and re-sampled to 3-mm isotropic voxels. After smoothing with an 8mm FWHM Gaussian kernel, the linear trend of time courses were removed. Then, the time series were transformed to the frequency domain using fast Fourier transform, the power spectrum was obtained. Since the power of a given frequency is proportional to the square of its amplitude in the original time series, the power spectrum obtained by fast Fourier transform was square root transformed, and then averaged across 0·01 to 0·08 Hz to yield a measure of ALFF from each voxel. For standardization purposes, the ALFF of each voxel was divided by the global mean ALFF value to standardize data across subjects.

Group comparisons

Voxel-by-voxel based comparisons of GMV and ALFF were performed between groups using two sample t-tests. For sub-group analyses, voxel-based comparisons of gray matter volume and the amplitude of low frequency fluctuation amongst the controls, and patient subgroups determined by negative symptom severity or illness duration, were performed using a one-way ANOVA followed by post hoc two-sample t-tests. The statistical results of GMV were corrected for multiple comparisons controlling for false discovery rate (FDR) and those of ALFF were corrected using the "AlphaSim" program implementation in REST software (2) based on the Monte Carlo simulation in AFNI software. (3) The AlphaSim program performs alpha probability simulations that are used to estimate the overall significance level (i.e. the probability of a false detection) for groups of voxels each individually meeting a significance threshold, rather than considering each voxel separately (4). This is accomplished by Monte Carlo simulation using the spatial correlation of voxels, voxel intensity thresholding, masking, and cluster identification. Based upon the combination of individual voxel probability thresholding and minimum cluster size thresholding, the probability of a false positive detection is determined. (4) We used a statistical threshold of $p<0·05$ corrected. To identify the association between structural abnormalities and clinical symptom severity, the average GMV and ALFF values of all voxels in abnormal areas revealed by VBM and ALFF were extracted and correlated with PANSS scores, age, and duration of illness using correlation analysis and then thresholded at $P < 0·05$. The MNI coordinates of our results were transformed to Talairach coordinates using mni2tal (http://imaging.mrc-cbu.cam.acuk/ down load /MNI2tal).

References

1. Good CD, Johnsrude IS, Ashburner J, Henson RN, Friston KJ, Frackowiak RS. A voxel-based morphometric study of ageing in 465 normal adult human brains. Neuroimage. 2001;14(1 Pt 1):21-36.

2. Song XW, Dong ZY, Long XY, Li SF, Zuo XN, Zhu CZ, He Y, Yan CG, Zang YF. REST: a toolkit for resting-state functional magnetic resonance imaging data processing. PLoS One. 2011;6(9):e25031.
3. Cox RW. AFNI: software for analysis and visualization of functional magnetic resonance neuroimages. Comput Biomed Res. 1996;29(3):162-73.
4. Xiong J, Gao JH, Lancaster JL, Fox PT. Clustered pixels analysis for functional MRI activation studies of the human brain. Human brain mapping. 1995;3(4):287-301.

FIGURE S1. Regions with altered gray matter volume or amplitude of low frequency fluctuation in drug-naive first episode schizophrenia.

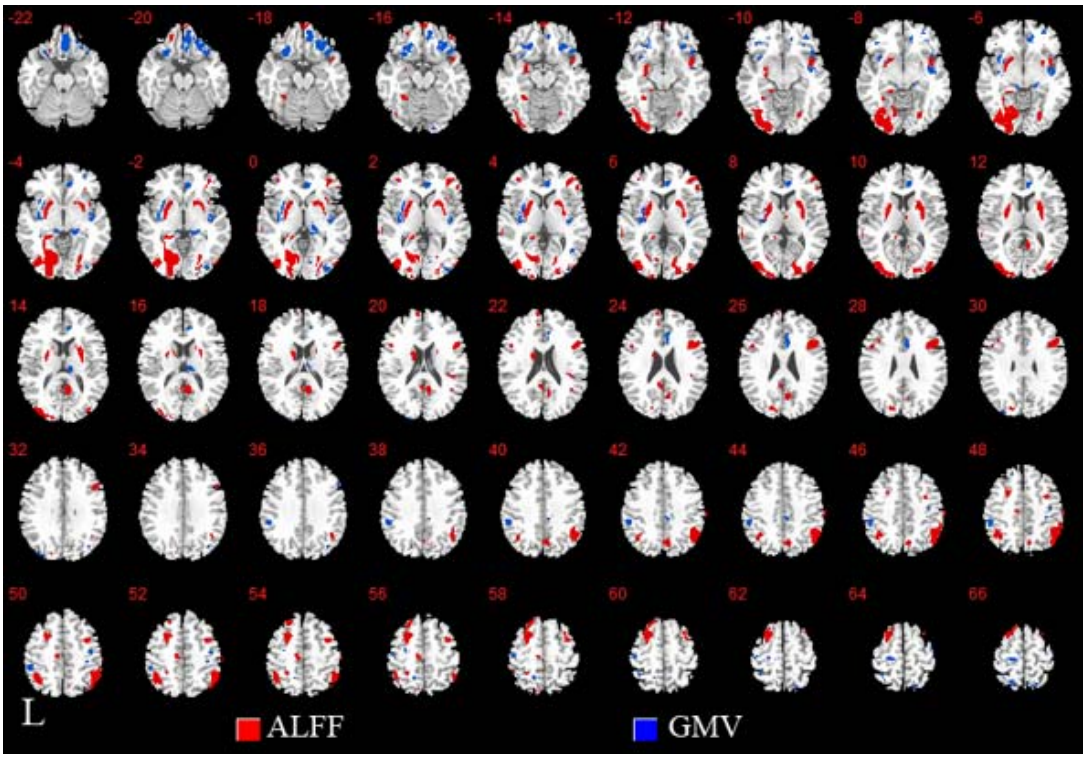

The regions in blue represents the altered gray matter volume in first episode schizophrenia, while those in red represents the altered amplitude of low frequency fluctuation in first episode schizophrenia. No overlapping was found between gray matter volume and amplitude of low frequency fluctuation. GMV: gray matter volume, ALFF: amplitude of low frequency fluctuation.

TABLE S1. Demographic and Clinical Characteristics for Antipsychotic-Naive First Episode Schizophrenia Patients and Healthy Controls.

Characteristic	Antipsychotic-Naïve First Episode Schizophrenia (N=100)	Controls (N=100)	
	Mean±SD	Mean±SD	P
Age (years)	24·30±7·45	24·39±7·58	0·87
Education (years)	12·32±3·02	13·15±2·45	0·10
Height (cm)	165.8 ± 7.9	163.4 ± 8.3	0.75
Weight (Kg)	63.4 ± 15.6	60.7 ± 13.2	0.54
Illness duration (months)	6·25±11·04	–	–
GAF score	28·72±10·75	–	–
PANSS scores			
Total	97·88±17·75	–	–
Negative symptoms	18·84±7·70	–	–
Positive symptoms	25·11±5·97	–	–
General psychopathology symptoms	47·63±9·61	–	–
Thought disturbance	13·94±3·77	–	–
Activation	9·26±3·22	–	–
Paranoid	10·43±2·86	–	–
Depression	9·11±4·48	–	–
Anergia	8·85±4·33	–	–
Impulsive aggression	15·99±5·26	–	–
	N	%	P
Gender(M/F)	41/59	41/59	–

TABLE S2. Differences of gray matter volume and amplitude of low frequency fluctuation amongst controls and drug-naïve first episode schizophrenia patients with and without prominent negative symptoms (P< 0.05 with correction for multiple comparisons).

Modality	Region	Coordinates			*Cluster size*	*t*
		x	*y*	*z*		
Gray matter volume	***Non-prominent* negative Patients>Controls**					
	Anterior cingulate	3	39	1	2307	4.28
	Left insula	-39	-4	1	644	4.12
	Right insula	39	15	10	267	3.61
	Bilateral thalamus	9	-31	-6	1731	5.23
	Left inferior frontal gyrus	-30	21	-20	118	4.03
	Controls>* Non-prominent *negative Patients					
	Right middle temporal gyrus	39	-57	4	253	5.22
	Right middle occipital gyrus	35	-87	-3	379	4.68
	Left postcentral gyrus	-45	-18	60	903	4.39
	Right medial frontal gyrus	9	68	-2	591	4.00
	Left middle frontal gyrus	-33	56	-14	408	3.75
	Prominent negative Patients>Controls					
	Right middle frontal gyrus	30	36	-21	317	4.4
	Left middle frontal gyrus	-24	44	-6	246	3.86
	Right insula	29	3	-12	137	4.18
	Left thalamus	-8	-22	13	125	3.93
	Right thalamus	9	-21	15	108	3.93
	Left insula	-36	3	3	246	3.82
	Left superior frontal gyrus	-11	59	27	737	4.51
	Right middle frontal gyrus	51	23	36	859	4.69
	Controls> Prominent negative Patients					
	Left inferior parietal lobule	-50	-36	49	677	3.83
	Right postcentral gyrus	27	-54	75	946	4.35
	Prominent negative Patients> Non-prominent negative Patients					
	Left middle frontal gyrus	-30	38	-23	294	3.95
	Left superior frontal gyrus	-12	61	28	392	3.99
	Right middle frontal gyrus	44	24	36	201	4.12
Amplitude of low frequency fluctuation	***Non-prominent* negative Patients>Controls**					
	Left putamen	-24	-3	15	188	4.65
	Right putamen	30	-3	-12	356	3.86
	Right cuneus	21	-84	3	132	4.24
	Left middle occipital gyrus	-24 .	-90	-6	390	4.29
	Controls>* Non-prominent *negative Patients					
	Left medial frontal gyrus	-1	60	-18	29	4.25
	Right middle frontal gyrus	45	18	30	39	3.77
	Left inferior parietal lobule	-42	-54	51	47	4.32
	Right inferior parietal lobule	45	-51	51	160	4.7
	Right middle frontal gyrus	36	3	54	23	4.32
	Left middle frontal gyrus	-24	12	60	145	5.11
	Prominent negative Patients>Controls					
	Left putamen	-24	-3	9	87	4.22
	Left posterior cingulate	-30	-69	9	87	4.07
	Left precuneus	-21	-69	30	32	3.65
	Right inferior parietal lobule	39	-36	24	12	3.72

Controls> Prominent negative Patients					
Right insula	39	9	-6	37	4.19
Left medial frontal gyrus	-9	54	21	33	3.72
Right inferior frontal gyrus	48	12	18	40	3.8
Right inferior parietal lobule	45	-54	48	55	4.19
Right parietal lobe	6	-63	45	20	3.77